Turkish Journal of Electrical Engineering & Computer Sciences

http://journals.tubitak.gov.tr/elektrik/

Research Article

Turk J Elec Eng & Comp Sci
(2019) 27: 1147 – 1156

doi:10.3906/elk-1802-76

Structure tensor adaptive total variation for image restoration

Surya PRASATH[1,2,3,4,*], **Dang Ngoc Hoang THANH**[5]

[1]Division of Biomedical Informatics, Cincinnati Children's Hospital Medical Center, Cincinnati, OH, USA
[2]Department of Pediatrics, University of Cincinnati, Cincinati, OH, USA
[3]Department of Biomedical Informatics, College of Medicine, University of Cincinnati, Cincinnati, OH, USA
[4]Department of Electrical Engineering and Computer Science, University of Cincinnati, Cincinnati, OH, USA
[5]Department of Information Technology, Hue College of Industry, Vietnam

Received: 09.02.2018 • **Accepted/Published Online:** 13.12.2018 • **Final Version:** 22.03.2019

Abstract: Image denoising and restoration is one of the basic requirements in many digital image processing systems. Variational regularization methods are widely used for removing noise without destroying edges that are important visual cues. This paper provides an adaptive version of the total variation regularization model that incorporates structure tensor eigenvalues for better edge preservation without creating blocky artifacts associated with gradient-based approaches. Experimental results on a variety of noisy images indicate that the proposed structure tensor adaptive total variation obtains promising results and compared with other methods, gets better structure preservation and robust noise removal.

Key words: Image restoration, total variation, adaptive, structure tensor, inverse gradient

1. Introduction

Image denoising and restoration are fundamental image processing steps due to the presence of random noise in digital imaging systems. Despite the improvements in various imaging sensors, noise is a nuisance that requires dedicated filters based upon the respective imaging system characteristics. There exists a large amount of denoising filters and variational and partial differential equation (PDE)-based image restoration methods [1] are widely utilized in many application domains where denoising is the preliminary requirement before deeper image analysis tasks, see [2] for more details. Among a wide variety of variational regularization models, two canonical regularizers are used for contrasting purposes, namely, the Tikhonov regularization that provides global smoothing, and total variation (TV) regularization first studied by Rudin et al. [3] for image restoration that obtains edge-preserving restorations.

Despite its edge-preserving property, TV regularization stimulated a lot of research due to its blocky artifact creation in homogeneous regions. Various adaptations and improvements were proposed over the last two decades with one of the main aims being to retain the edge preservation property while alleviating the blocky artifacts in the resultant images [4–6]. Strong and Chan [7] provided one of the earliest attempts in this direction by augmenting a weight function that depends on spatial pixel locations to guide the total variation regularization with edges. By using a smoothed inverse gradient-based indicator function, these weighted TV models provide better restoration results than the classical TV regularization, though similar block artifacts can manifest as the gradient computations are prone to noise, see Figure 1. Figure 1a shows a noisy grayscale

*Correspondence: surya.prasath@cchmc.org, prasatsa@uc.edu

(a) Input (b) Inverse gradient weight (c) Structure tensor weight

Figure 1. Using edge indicator-based weights, our adaptive TV regularization provides better noise removal without smoothing out the edges. a) Input *House* grayscale 256×256 test image with Gaussian noise $\sigma_n = 30$, b) weight function computed using the inverse gradient of the input image, see Eq. (5) with parameters $k = 20$, $\sigma = 1$, and c) weight function computed using the proposed structure tensor eigenvalues of the input image, see Eq. (7), with parameters $\epsilon = 0.05$, $\sigma = 1$. Both weights were inverted and rescaled to $[0, 1]$ for better visualization.

input image, Figure 1b shows the typical inverse gradient-based weight map, and Figure 1c shows the proposed structure tensor-based weight map indicating better edge differentiation under noise. More sophisticated choices for the adaptive parameter within TV regularization have been considered before. For example, a local variation estimation [6] with a split Bregman algorithm-based implementation [8] was considered. In this work, we advocate the use of structure tensor-based eigenvalues that are useful in computing noise-robust features in digital images. Structure tensor and their eigenanalysis has been used for denoising [9], flow enhancement [10], and many other computer vision problems. We use a structure tensor adaptive total variation (STATV) for a better weight function that can guide the TV regularization, which can avoid the artifacts and improve upon the previous adaptive models. There are two key differences between our current approach and [6]. First, the previous method utilizes a local variance-based adaptive parameter estimation within TV regularization that do not incorporate structural variations. These can be captured by structure tensor eigenvalues-based adaptive parameter. Second, the multiscale nature of our proposed structure tensor-based parameter can retain small-scale details that cannot be kept in the local variation parameter. Experimental results on various noisy images are undertaken and comparison with previous regularization models are given with respect to peak signal to noise ratio, structural similarity, and an edge-based error metrics.

The rest of the paper is organized as follows. Section 2 introduces the proposed method in terms of the total variation regularization. Section 3 provides experimental results on noisy images as well as comparisons with other related methods from the literature. Finally, Section 4 concludes the paper.

2. Structure tensor adaptive total variation

We introduce a structure tensor eigenvalues-based weight function that can be adaptively used in the TV regularization for image restoration with effective noise removal and edges preservation.

2.1. Structure tensor

Let $u : \Omega \to \mathbb{R}$ be a grayscale image, that is $u(x, y)$ is the pixel value at the spatial location $(x, y) \in \Omega$ of the image domain $\Omega \subset \mathbb{R}^2$, a rectangle. The structure tensor is a 2×2 matrix computed at every pixel $(x, y) \in \Omega$

and is given by,

$$K_\sigma(u(x,y)) = G_\sigma \star (\nabla u \, \nabla u^T) \tag{1}$$

$$= \begin{bmatrix} G_\sigma \star u_x^2 & G_\sigma \star u_x u_y \\ G_\sigma \star u_y u_x & G_\sigma \star u_y^2 \end{bmatrix}, \tag{2}$$

where $\nabla u = (u_x, u_y)$ is the gradient of the image u, and superscript T is the vector transpose. Here, the convolution $\star$ with a 2D Gaussian low-pass filter $G_\sigma(x,y) = (\sigma\sqrt{2\pi})^{-1} \exp\left(-(x^2+y^2)/2\sigma^2\right)$ is undertaken to avoid the ill-posedness of gradient components under noisy conditions. The structure tensor entries are positive and the matrix K_σ is symmetric and positive semidefinite provided that there are enough gradient samples in the neighborhood. Let the eigenvalues of Eq. (1) be $(\lambda_+(x,y,\sigma),\ \lambda_-(x,y,\sigma))$ which are the maximum and minimum, respectively, and $\lambda_+ \geq \lambda_-$ (from here on we drop the spatial (x,y) and scale (σ) dependency in our notations for simplicity). The eigenvalues encode local information on σ neighborhood and can provide robust feature detections that can be utilized for low-level image processing steps [9, 10]. This can be seen in an example image, see Figure 2. In Figures 2a–2c, we show the components of the smoothed structure tensor entries respectively. Figure 2d shows the tensor field visualization with each point in the image is an ellipse with long axis λ_+, the minor axis λ_-.

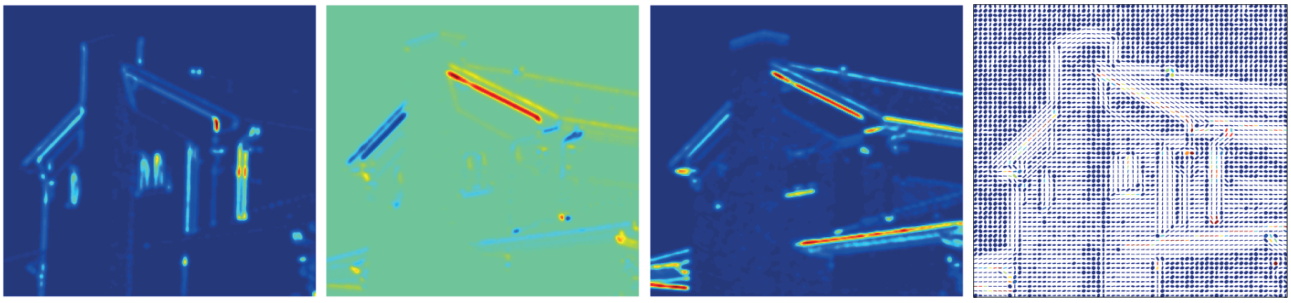

(a) $G_\sigma \ast u_x^2$ (b) $G_\sigma \ast u_x u_y$ (c) $G_\sigma \ast u_y^2$ (d) Structure tensor

Figure 2. Smoothed structure tensor entries capture the image discontinuities. We show the structure tensor entries on the *House* grayscale test image. (a) $G_\sigma \star u_x^2$, (b) $G_\sigma \star u_x u_y$, (c) $G_\sigma \star u_y^2$, and (d) the structure tensor visualized as a tensor field where each point is an ellipse with the long axis λ_+, the minor axis λ_-. The pre-smoothing parameter for the convolution with the Gaussian filter is $\sigma = 1$.

2.2. Adaptive total variation

In this work, we utilize the adaptive total variation (ATV) regularization,

$$\min_u \left\{ \int_\Omega \Phi(|\nabla u|)\, dx + \int_\Omega (u - u_0)\, dx, \right\} \tag{3}$$

with the weight based edge indicator functions,

$$\Phi(|\nabla u|) = \omega\, |\nabla u|\,. \tag{4}$$

Note here that we assume an additive Gaussian noise-corrupted image is given, that is, $u_0 = u + n$, where u_0 is the input noisy image, u is the original (unknown) true image that we are trying to find and $n \sim \mathcal{N}(0, \sigma_n^2)$ the

normalized Gaussian noise with zero mean and σ_n standard deviation. The spatially adaptive weight function ω is chosen typically as smoothed inverse gradient [7, 11],

$$\omega := \frac{1}{1 + k\ |G_\sigma \star \nabla u|}, \tag{5}$$

with $k > 0$ a contrast parameter. However, this inherits some of the drawbacks with other gradient regularizations such as detecting blocky edges, see Figure 1b. To improve the performance of the weighted TV regularization, and to avoid blocky artifacts, here we propose the following structure tensor-based weight function that incorporates the eigenvalues for better edge guidance than gradients. We consider the following exponent function based on the eigenvalues of the structure tensor,

$$p = \exp\left[-\left(\frac{\lambda_+\ \lambda_-}{\epsilon + \lambda_+ + \lambda_-}\right)^2\right] \exp\left[-\left(\frac{\lambda_+ - \lambda_-}{\epsilon + \lambda_+ + \lambda_-}\right)^2\right], \tag{6}$$

where a small parameter $\epsilon > 0$ is added for numerical stability. Note that we use the shortened notation p to denote the function $p(x, y, \sigma)$ where the eigenvalues of the structure tensor matrix in Eq. (1) are computed for a particular scale $\sigma > 0$ at the pixel location $(x, y) \in \Omega$. We converted the eigenvalues $(\lambda_+,\ \lambda_-)$ to be in $[0, 1]$ range by rescaling to avoid the negative values, since we require a weight map that depends on the absolute values to capture edge information from p in Eq. (6), and set $\epsilon = 0.05$ in the experiments. The multiplication of $(\lambda_+,\ \lambda_-)$-based term (the first exponential term in Eq. (6)) is the harmonic mean of the eigenvalues, and captures corners in the image that contains high spatial frequencies. The subtraction of $(\lambda_+,\ \lambda_-)$-based term (the second exponential term in Eq. (6)) is the coherence measure and captures the edge information. We next define our weight function as a spatially varying multifeature map,

$$\omega := \frac{1}{1 + k\ |p|}, \tag{7}$$

where $k > 0$ as before a parameter. We can use the multiscale structure tensor-based map in (6) via the weight function in (7) as a guide to the TV-based image restoration in Eq. (4) with better edges preservation. Due to its robustness to noise, see Figure 1c, this map is used as an edge indicator function in TV image restoration method in Eq. (3), called structure tensor adaptive total variation (STATV), obtains better restoration results as we will in the experimental results (Section 3). There exist many convergent numerical implementations [12] for the TV regularization that can be adapted for the ATV model considered here. However, we utilize the well-known split Bregman algorithm [8] to solve the adaptive TV regularization in Eq. (3) here due to its efficiency.

3. Experimental results

3.1. Setup

The following parameters are fixed for all the experiments reported here. We used the parameter $k = 20$ in both the adaptive TV [7] and our proposed STATV models, $\epsilon = 0.05$ in Eq. (6) and the presmoothing parameter $\sigma = 1$ for the convolution with the Gaussian are used in both the inverse gradient weight function in Eq. (5) and the structure tensor components in Eq. (1). For the method in [4], the default parameters are used, and the iteration time of all the methods is determined by the highest PSNR (dB) values.

3.2. Comparison results

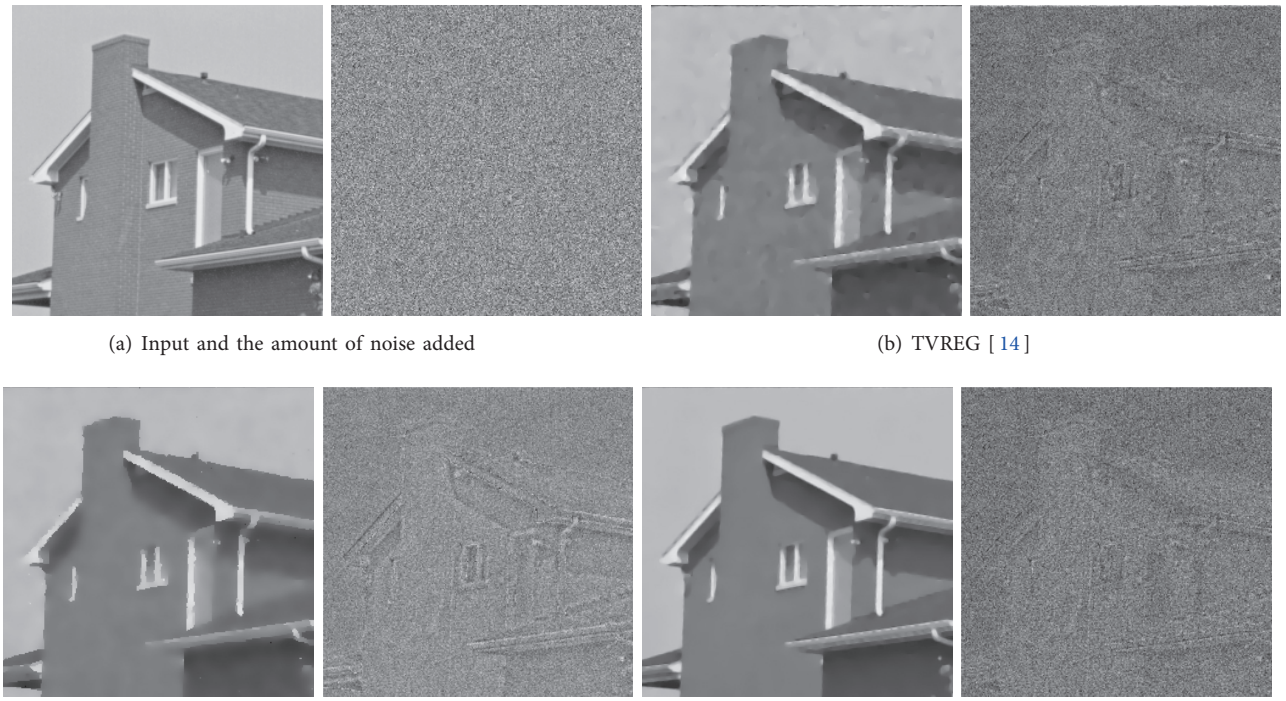

(a) Input and the amount of noise added

(b) TVREG [14]

(c) APMAD [4]

(d) Our STATV

Figure 3. Our proposed method works better than the related regularization models by removing noise and preserving edges without blocky artifacts. a) Denoising results along with method noise images obtained with b) total variation (TVREG) [3], c) adaptive Perona-Malik (APMAD) [4], and d) our proposed STATV. In each row, we show the denoised result (left) along with the method noise $|u_{\text{Noisy}} - u_{\text{Denoised}}|$ (right) indicating the amount of noise removed by each method.

Figure 3 shows a comparison of different regularization methods on a noisy *House* grayscale test image (input image with Gaussian noise $\sigma_n = 30$ is shown in Figure 1a. In Figure 3a, we show the latent (unknown) true image, the amount of noise added, and subsequently the denoising results with total variation regularization (TVREG) [3], adaptive Perona–Malik anisotropic diffusion (APMAD) [4], and our proposed STATV with respective method noise ($|u_{\text{Noisy}} - u_{\text{Denoised}}|$ indicates the amount of noise removed by the method). As can be seen, the TVREG result in Figure 3b shows considerable staircasing/block artifacts in homogeneous areas, whereas the APMAD result in Figure 3c, though better than the TVREG, still inherits the blocky artifacts. In contrast, our STATV results in Figure 3d shows an overall better edge preservation without any of the aforementioned artifacts. Moreover, comparing the method noise images, we see that our STATV removes noise without affecting the overall edges and salient structures. In particular, better edge preservation can be observed in structure tensor eigenvalues-based total variation result (Figure 3d) than with inverse gradient-based total variation result (Figure 3b).

Next, in Figure 4a, we show a partially textured *Baboon* grayscale test image, and in Figure 4b, a corrupted version by Gaussian noise $\sigma_n = 30$. Figure 5 shows the denoising results with TVREG, adaptive TV (ATVREG) [7], and our proposed STATV methods. It is clear that our proposed STATV method obtains better edge preservation while the TVREG and ATVREG models obtain staircasing artifacts. This can be seen on the cropped versions (mouth, eye) of the denoised results, TVREG (Figure 5a) and ATVREG (Figure 5b) both

(a) Original

(b) Noisy

Figure 4. Original and noise versions of the *Baboon* grayscale 256×256 test image with Gaussian noise $\sigma_n = 30$ used in our denoising comparisons. a) original, and b) noisy images. In each row, we show the image (left) along with the cropped parts of the image (middle, right).

either oversmooth or create staircasing artifacts, whereas our proposed STATV (Figure 5c) keeps the majority of edges without oversmoothing and has no visible artifacts. To further compare the image denoising results from different filters quantitatively, we utilize three error measures including two well-known standard error metrics, namely the peak signal-to-noise ratio (PSNR, measured in decibels - dB), and the mean structural similarity (MSSIM, varies in the range $[0, 1]$ with 0-low, 1-high quality). These two are the image quality metrics widely used in image processing literature for comparing the quality of restoration with the known reference image (original/noise-free). Along with these, we use a new metric ($\mathrm{PSNR_E}$) based on gradient edge maps that can capture the edge preservation quality between different methods.

1. **PSNR**: Peak signal-to-noise ratio which is given in decibels (dB). Higher PSNR value indicates optimum denoising capability. PSNR for a denoised image $\tilde{u}$ is given by,

$$\mathrm{PSNR}(\tilde{u}) = 20 * \log_{10}\left(\frac{\tilde{u}_{max}}{\sqrt{\mathrm{MSE}}}\right) dB, \tag{8}$$

   where $\mathrm{MSE} = (mn)^{-1} \sum\sum (\tilde{u} - u)^2$, with u is the original (noise free) image, $m \times n$ denotes the image size, $\tilde{u}_{max}$ denotes the maximum value, for example in 8-bit images $\tilde{u}_{max} = 255$. A difference of $0.5\,dB$ can be identified visually.

2. **$\mathrm{PSNR_E}$**: Following [4], we use the PSNR of the edge maps (EM), $\mathrm{EM}(\xi) = 2 - (2/(1 + k\,|\nabla G_\sigma \star \xi|^2)$ with $k = 0.0025$, $\sigma = 0.5$.

$$\mathrm{PSNR_E}(\tilde{u}) = 20 * \log_{10}\left(\frac{\max \mathrm{EM}(u) - \min \mathrm{EM}(u)}{\mathrm{MSE_E}}\right) dB, \tag{9}$$

(a) TVREG [14]

(b) ATVREG [15]

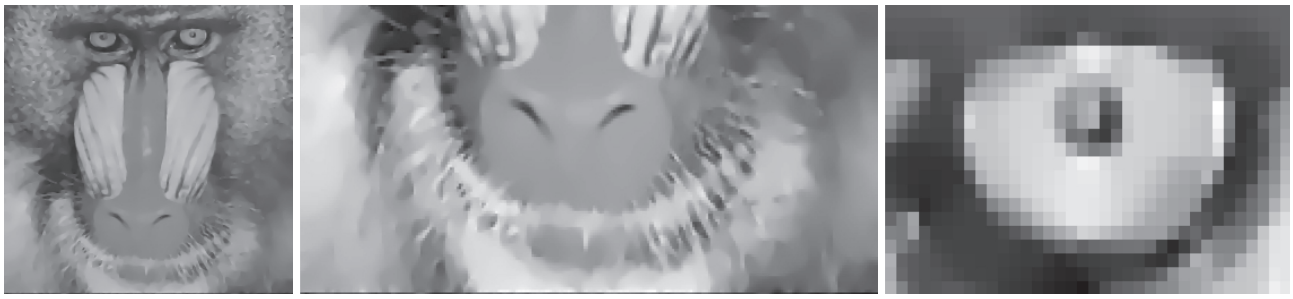

(c) Our STATV

Figure 5. Our proposed method works better than the other classical and adaptive TV regularization models. Denoising applied on a noisy version (Gaussian noise $\sigma_n = 30$ added) obtained with: a) total variation (TVREG) [3], b) adaptive TV (ATVREG) [7], and c) our proposed STATV. In each row, we show the image (left) along with the cropped parts of the image (middle, right).

where $\mathrm{MSE_E} = (mn)^{-1} \sum\sum(\mathrm{EM}(\tilde{u}) - \mathrm{EM}(u))^2$. Higher $\mathrm{PSNR_E}$ indicates that the method performs better edge preservation by way of matching the derivatives.

3. **MSSIM**: Mean structural similarity (MSSIM) index is in the range $[0, 1]$ and is known to be a better error metric than the traditional signal-to-noise ratio [13]. It is the mean value of the structural similarity (SSIM) metric. The SSIM is calculated between two windows ω_1 and ω_2 of common size $N \times N$, and is given by,

$$\mathrm{SSIM}(\omega_1, \omega_2) = \frac{(2\mu_{\omega_1}\mu_{\omega_2} + c_1)(2\sigma_{\omega_1\omega_2} + c_2)}{(\mu_{\omega_1}^2 + \mu_{\omega_2}^2 + c_1)(\sigma_{\omega_1}^2 + \sigma_{\omega_2}^2 + c_2)}, \tag{10}$$

where μ_{ω_i} is the average of ω_i, $\sigma_{\omega_i}^2$ is the variance of ω_i, $\sigma_{\omega_1\omega_2}$ is the covariance, and c_1, c_2 are stabilization parameters. We use the default parameters for SSIM. The MSSIM value near 1 implies the optimal denoising capability of a method and we used the default parameters.

Table 1 shows the PSNR, and PSNR_E (dB) values for various regularization methods compared with our proposed STATV in different standard test images taken from the USC-SIPI Miscellaneous dataset. The images are corrupted with Gaussian noise of strength $\sigma_n = 30$. Overall, our approach obtains the highest PSNR, PSNR_E values indicating better signal and edge preservation, respectively. Table 2 shows the MSSIM values. Higher MSSIM values show that our denoised images are structurally similar to the original noise-free images showcasing good fidelity.

Table 1. $\text{PSNR}/\text{PSNR}_\text{E}$ (dB) comparison of various methods for standard test images from USC-SIPI Miscellaneous dataset. Noisy image is obtained by adding Gaussian noise of strength $\sigma_n = 30$ to the original image. Each column indicates the $\text{PSNR}/\text{PSNR}_\text{E}$ (dB) values for different test images. Best results are in **boldface**.

Images	TVREG [3]	ATVREG [7]	APMAD [4]	Our STATV
Couple	29.89 14.58	30.35 14.88	28.40 12.61	**31.83** **17.25**
F-16	25.72 10.57	26.01 10.73	24.22 8.45	**27.91** **14.17**
Girl1	29.63 14.29	29.78 14.70	27.90 12.50	**31.35** **16.76**
Girl2	31.03 16.61	31.60 16.98	29.59 14.55	**33.73** **20.07**
Girl3	30.30 15.10	31.25 15.45	28.07 12.95	**33.04** **18.85**
House	29.50 15.18	30.08 15.81	27.49 12.75	**31.53** **19.58**
IPI	31.37 15.89	32.18 16.76	29.25 14.00	**34.82** **19.63**
IPIC	30.32 15.03	31.17 16.05	27.58 12.77	**33.75** **19.03**
Tree	25.45 10.35	25.76 10.80	23.71 8.38	**27.60** **13.73**
Baboon	22.81 6.27	22.52 6.03	21.85 4.87	**23.35** **9.27**
Barbara	25.31 10.70	25.41 10.82	23.81 8.67	**25.75** **13.35**
Boat	25.57 9.78	25.69 9.98	24.09 7.92	**27.07** **12.32**
Car	24.76 8.65	24.91 8.83	23.33 6.89	**26.42** **11.45**
Lena	26.72 11.31	26.92 11.56	24.86 9.40	**28.63** **14.26**
Peppers	28.16 12.87	28.49 13.21	25.98 10.72	**30.81** **16.48**
Splash	30.59 15.59	31.51 15.92	28.30 13.08	**34.24** **20.32**
Tiffany	27.57 11.36	27.65 11.35	25.66 9.45	**29.39** **14.35**

Despite good denoising results with edges preservation, our proposed STATV removes small-scale texture details and will not be suitable for preserving partially textured images, for example, see the *Baboon* denoising result in Figure 5 where the whiskers and the side regions are smoothed out, also in the *House* in Figure 3 on the roof and tiles. This property is true for any variational and PDE-based models due to global smoothing nature and a separate texture modeling will be required to alleviate this effect.

4. Conclusion

Image restoration with adaptive weight-based total variation regularization model is proposed in this work. Instead of noise-prone inverse gradient-based weights typically used in the literature, we employed eigenanalysis of the structure tensor that is robust against noise and provides a better guideline edge map. Total variation regularization combined with the power of structure tensor adaptiveness provided better edge preserving image denoising and comparisons with related works showed that the proposed approach is better-suited for restoration

Table 2. MSSIM comparison of various methods for standard test images from USC-SIPI Miscellaneous dataset. Noisy image is obtained by adding Gaussian noise of strength $\sigma_n = 30$ to the original image. Each column indicates the MSSIM values for different test images. Best results are in **boldface**.

Images	TVREG [3]	ATVREG [7]	APMAD [4]	Our STATV
Couple	0.7620	0.7748	0.7190	**0.8407**
F-16	0.8015	0.8103	0.7572	**0.8598**
Girl1	0.8011	0.8068	0.7522	**0.8543**
Girl2	0.8844	0.8877	0.8694	**0.8867**
Girl3	0.8576	0.8646	0.8195	**0.8880**
House	0.8145	0.8199	0.7860	**0.8365**
IPI	0.9223	0.9322	0.9092	**0.9438**
IPIC	0.9109	0.9218	0.8782	**0.9372**
Tree	0.7739	0.7816	0.7189	**0.8374**
Baboon	0.4951	0.4688	0.3825	**0.6591**
Barbara	0.7005	0.7034	0.6282	**0.7631**
Boat	0.6959	0.6947	0.6154	**0.7904**
Car	0.7187	0.7225	0.6409	**0.8139**
Lena	0.7853	0.7904	0.7250	**0.8485**
Peppers	0.8343	0.8408	0.7833	**0.8927**
Splash	0.8908	0.9018	0.8711	**0.9119**
Tiffany	0.7627	0.7646	0.6897	**0.8333**

under different noise levels. Extending the proposed model to handle mixed noise removal [14–18] and color images [19, 20] defines our future works.

References

[1] Perona P, Malik J. Scale-space and edge detection using anisotropic diffusion. IEEE Transactions on Pattern Analysis and Machine Intelligence 1990; 12: 629-639. https://doi.org/10.1109/34.56205

[2] Aubert G, Kornprobst P. Mathematical Problems in Image Processing: Partial differential Equation and Calculus of Variations. New York, NY, USA: Springer-Verlag, 2006.

[3] Rudin L, Osher S, Fatemi E. Nonlinear total variation based noise removal algorithms. Physica D 1992; 60: 259-268. https://doi.org/10.1016/0167-2789(92)90242-F

[4] Guo Z, Sun J Zhang, D, Wu B. Adaptive Perona-Malik model based on the variable exponent for image denoising. IEEE Transactions on Image Processing 2012; 21: 958-967.

[5] Prasath VBS, Vorotnikov D. Weighted and well-balanced anisotropic diffusion scheme for image denoising and restoration. Nonlinear Analysis: Real World Applications 2014; 17: 33-46. https://doi.org/10.1016/j.nonrwa.2013.10.004

[6] Prasath VBS, Thanh DNH, Hai NH, Cuong NX. Image restoration with total variation and iterative regularization parameter estimation. In: The Eighth International Symposium on Information and Communication Technology (SoICT); 2017; Nha Trang, Vietnam. New York, NY, USA: ACM. pp. 378-384. https://doi.org/10.1145/3155133.3155191

[7] Strong DM, Chan TF. Spatially and scale adaptive total variation based regularization and anisotropic diffusion in image processing. Technical Report 96-46, UCLA CAM, 1996.

[8] Goldstein T, Osher S. The split Bregman algorithm for L1 regularized problems. SIAM Journal on Imaging Sciences 2009; 2: 323-343. https://doi.org/10.1137/080725891

[9] Prasath VBS, Vorotnikov D, Pelapur R, Jose S, Seetharaman G, Palaniappan K. Multiscale Tikhonov-total variation image restoration using spatially varying edge coherence exponent. IEEE Transactions on Image Processing 2015; 24: 5220-5235. https://doi.org/10.1109/TIP.2015.2479471

[10] Prasath VBS. Adaptive coherence-enhancing diffusion flow for color images. Informatica 2016; 40: 337-342.

[11] Prasath VBS, Singh A. An adaptive anisotropic diffusion scheme for image restoration and selective smoothing. International Journal of Image and Graphics 2012; 12: 18pp. https://doi.org/10.1142/S0219467812500039

[12] Prasath VBS. On convergent finite difference schemes for variational - PDE based image processing. Computational and Applied Mathematics 2018; 37: 1562-1580. https://doi.org/10.1007/s40314-016-0414-9

[13] Wang Z, Bovik AC, Sheikh HR, Simoncelli EP. Image quality assessment: from error visibility to structural similarity. IEEE Transactions on Image Processing 2004; 13: 600-612. https://doi.org/10.1109/TIP.2003.819861

[14] Thanh, DNH, Dvoenko SD, Sang DV. A mixed noise removal method based on total variation. Informatica 2016; 40: 159-167.

[15] Erkan U, Gökrem L. A new method based on pixel density in salt and pepper noise removal. Turk J Elec Eng & Comp Sci 2018; 26: 162-171. https://doi.org/10.3906/elk-1705-256

[16] Thanh DNH, Dvoenko SD. A method of total variation to remove the mixed Poisson-Gaussian noise. Pattern Recognition and Image Analysis 2016; 26: 285-293. https://doi.org/10.1134/S1054661816020231

[17] Thanh D, Dvoenko S, Sang D. A denoising method based on total variation. In: The Sixth International Symposium on Information and Communication Technology (SoICT); 2015; Hue City, Viet Nam. New York, NY, USA: ACM. pp. 223-230. https://doi.org/10.1145/2833258.2833281

[18] Thanh DNH, Prasath VBS, Hieu LM. A review on CT and X-ray images denoising methods. Informatica 2019; 43: 9pp.

[19] Prasath VBS, Singh A. Multispectral image denoising by well-posed anisotropic diffusion scheme with channel coupling. International Journal of Remote Sensing 2010; 31: 2091-2099. https://doi.org/10.1080/01431160903260965

[20] Moreno JC, Prasath VBS, Neves JC. Color image processing by vectorial total variation with gradient channels coupling. Inverse Problems and Imaging 2016; 10: 461-497.